JMEPEG (2006) 15:230-235
DOI: 10.1361/105994906X95931

1059-9495/$19.00

Human Microvascular Endothelial Cell Seeding on Cr-DLC Thin Films for Heart Valve Applications

N. Ali, Y. Kousar, J. Gracio, E. Titus, T.I. Okpalugo, V. Singh, M. Pease, A.A. Ogwu, E.I. Meletis, W. Ahmed, and M.J. Jackson

(Submitted November 4, 2005; in revised form December 24, 2005)

In this investigation, Cr-modified diamond-like carbon (Cr-DLC) films were studied for potential applications in mechanical heart valves. Three Cr-DLC samples were prepared using a magnetron sputtering technique employing an intensified plasma-assisted processing (IPAP) system. The three samples consisted of the following Cr contents: 1, 5, and 10 at.%. The biological response of human microvascular endothelial cells (HMV-EC), seeded on Cr-DLC films, was evaluated in terms of initial cell attachment and growth. The Cr-DLC films were characterized using Raman spectroscopy, x-ray diffraction, scanning electron microscopy, secondary ion mass spectroscopy, and by the contact angle technique. Endothelial cell adhesion and growth were found to be affected by changing the Cr content of Cr-DLC films.

Keywords endothelial cells, hemocompatibility, heart valves, metal-DLC

1. Introduction

The failure of heart valves accounts for about 25 to 30% of heart problems that occur today. Faulty heart valves need to be replaced by artificial ones via sophisticated and sometimes risky surgery. However, once a heart valve has been replaced with an artificial one, it is desirable that it lasts the life span of the patient. Therefore, any technique that can improve the operational life of prosthetic heart valves is highly desirable. Pyrolytic carbon (PyC) is widely used for the manufacture of mechanical heart valves. Although it has widespread usage for heart-valve purposes, PyC is not the ideal material. In its processed form, PyC is a ceramic-like material, and thus it is subject to brittleness. Therefore, if a crack appears, the material, like glass, has very little resistance to the growth/propagation of the crack and may fail under stress. In addition, its blood compatibility is not ideal for prolonged clinical use. As a result, thrombosis often occurs in patients who are required to take anticoagulation drugs on a regular basis (Ref 1). Anticoagulation therapy can give rise to some serious side effects, such as birth defects. It is, therefore, extremely important to develop new materials that have better surface characteristics, blood compatibility, improved wear resistance, and toughness. Although there has been comparatively less work reported on the surface engineering of mechanical heart valves, a number of researchers have attempted to develop biocompatible coatings, which could potentially be used for artificial heart valves. For example, carbon nitride (CN) thin films have been investigated for biocompatibility, and their properties strongly suggest their potentials for use in various surgical implants (Ref 2). Generally, both the bio- and hemocompatibility of DLC coatings have been extensively investigated and widely reported in the open literature (Ref 3). Jones et al. (Ref 4) deposited DLC coatings, consisting of multilayers of TiC and TiN, onto Ti substrates and characterized the coatings for hemocompatibility, thrombogenicity, and interactions with rabbit blood platelets. It was found that DLC produced no hemolytic effect, platelet activation, or tendency toward thrombus formation. Furthermore, the platelet spreading correlated with the surface energy of the coatings. Thomson et al. (Ref 5) and Dion et al. (Ref 6) have also investigated DLC coatings and characterized their biological properties. Okpalugo et al. (Ref 7) studied the hemocompatibility properties and endothelial cell seeding behavior of Si-DLC and thermally annealed Si-DLC films. The results showed that silicon incorporation in DLC improved the hemocompatibility properties and improved seeding of endothelial cells onto Si-DLC surfaces. Furthermore, thermally annealing Si-DLC films improved the endothelial cell seeding efficiency. Yang et al. (Ref 8) deposited Ti-O thin films using plasma-immersion ion-implantation technique and characterized the anticoagulant property employing in-vivo methods. They found that the Ti-O film coatings exhibited better thromboresistant properties than did low-temperature isotropic carbon (LTIC) in long-term implantation. Chen et al. (Ref 9) deposited TiO coatings doped with Ta, using magnetron sputtering and thermal oxidation procedures and studied the antithrombogenic and hemocompatibility of $Ti(Ta^{+5})O_2$ thin films. The blood compatibility was measured in vitro using blood clotting and platelet adhesion measurements. The films were found to exhibit attractive blood compatibility exceeding that of LTIC. Leng et al. (Ref 10) investigated the biomedical properties of tantalum nitride (TaN) thin films. They showed that the blood compatibility of TaN films was superior to other common biocompatible coatings, such as TiN, Ta, and LTIC. Potential heart valve duplex coatings, con-

This paper was presented at the fourth International Surface Engineering Congress and Exposition held August 1-3, 2005 in St. Paul, MN.

N. Ali, Y. Kousar, J. Gracio, and **E. Titus,** Centre for Mechanical Technology and Automation, University of Aveiro, Portugal; **T.I. Okpalugo,** Northern Ireland Bio-Engineering Centre, NIBEC, University of Ulster, U.K.; **V. Singh** and **M. Pease,** Center for Advanced Microstructures and Devices, Louisiana State University, Baton Rouge, LA 70806; **A.A. Ogwu,** Thin Film Centre, University of Paisley, Scotland, U.K.; **E.I. Meletis,** Materials Science and Engineering, The University of Texas at Arlington, Arlington, TX; and **W. Ahmed** and **M.J. Jackson,** Department of Mechanical Engineering, College of Technology, Purdue University, West Lafayette, IN 47907-2021. Contact e-mail: jacksomj@purdue.edu.

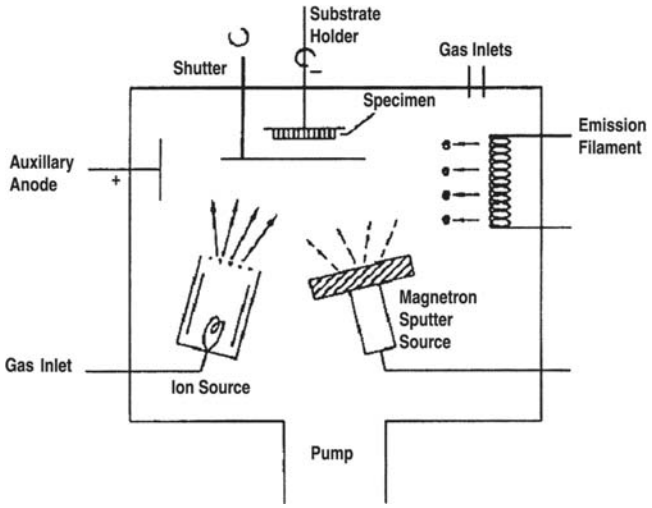

Fig. 1 Schematic of the IPAP thin film deposition system with triode configuration

sisting of layers of Ti-O and Ti-N, have been deposited onto biomedical Ti-alloy by Leng et al. (Ref 11), and their blood compatibility and mechanical properties have been characterized. The TiO layer was designed to improve the blood compatibility, whereas TiN was deposited to improve the mechanical properties of the TiO/TiN duplex coatings. They found that the duplex coatings displayed (a) better blood compatibility than LTIC; (b) greater microhardness; and (c) improved wear resistance than Ti_6Al_4V alloys. It has been reported that the TiO coatings display superior blood compatibility to LTIC (Ref 12). For narrow-diameter synthetic grafts (<6 mm) and other potential blood-contacting devices that are thrombogenic, the current trend is to apply cell seeding of the endothelial cells onto the surfaces to reduce thrombogenicity (Ref 13). The endothelial lining has also been reported to be the best nonthrombogenic surface (Ref 14). Current investigations are aimed at evaluating the potential of a more readily available synthetic Cr-modified diamond-like carbon (Cr-DLC) film for thromboresistant applications. This has promising future applications involving possible in-vitro growth of endothelial cells on Cr-DLC-coated devices before the implantation of such devices in the human body. It has also been stated that the biocompatibility of materials can be influenced by factors such as hydrophobicity and topography (Ref 15, 16). The hydrophilic or hydrophobic nature of a surface has also been associated with the extent of cell interactions with the surface (Ref 17, 18).

In this paper, three types of Cr-DLC films were deposited onto 50 mm circular silicon wafers using magnetron sputtering utilizing the IPAP system (Fig. 1). The films were deposited so that the Cr content in each film was kept at (a) 1, (b) 5, and (c) 10 at.%. There are no reports, to the knowledge of the authors, on Cr-DLC surfaces seeded with HMV-EC. The as-deposited Cr-DLC films were characterized for physical properties using a number of techniques, including Raman spectroscopy (RS), x-ray diffraction (XRD), scanning electron microscopy (SEM), and secondary ion mass spectroscopy (SIMS) analysis.

2. Experimental Procedures

2.1 Cr-DLC Deposition

Cr-DLC films were deposited onto silicon (100) wafer, with a diameter of 50 mm, in a surface modification system capable of operating in three different modes, namely, conventional (diode) and intensified (triode) plasma-enhanced processing, ion-beam-assisted deposition/treatment, and magnetron sputter deposition. Detailed information on this process can be found elsewhere (Ref 19). Figure 1 shows the schematic diagram of the system used to prepare the Cr-DLC film samples. The films were synthesized using a hybrid technique involving physical vapor deposition (PVD) and plasma-enhanced chemical vapor deposition. The substrate after cleaning was mounted in the chamber, which was evacuated down to 1.33×10^{-4} Pa and purged with Ar several times. Subsequently, the Si substrate was sputter cleaned using Ar^+ for ~20 min at 3.3 Pa chamber pressure and −1500 V bias voltage. Films were synthesized by sputtering of a Cr target (99.5% Cr) in a CH_4/Ar gas discharge (ratio of 1:5.33) and total flow rate of 47.5 sccm. Cr content in the films was controlled by running the magnetron in the current control mode and modulating the current. The chamber pressure was maintained at 2.66 Pa as the optimal pressure. Table 1 displays the deposition conditions used to deposit the Cr-DLC films. After processing, the substrate was cooled inside the chamber in an Ar atmosphere. The substrate temperature during deposition remained less than 100 °C.

Table 1 Deposition parameters employed in depositing Cr-DLC films using the IPAP process

Sample	Deposition rate, nm/min	Magnetron current, mA
1 at.% Cr-DLC	6.6	155
5 at.% Cr-DLC	7.6	220
10 at.% Cr-DLC	15.2	310

Bias voltage, −1000 V; flow rate (sccm), CH_4:Ar 7.4:40; chamber pressure, 2.66 Pa; processing time, 2 h; sputter cleaning, Ar^+:3.3 Pa, −1500 V, ~20 min

2.2 Microstructure Characterization

Raman measurements were performed on the Cr-DLC samples at room temperature using an ISA JOBIN YVON-SPEX T64000 (Edison, NJ) Raman spectrometer equipped with an Ar-ion laser at 514.53 nm to determine the types of carbon phases. The appropriate filter for spectra acquisition was then selected and the spectra acquired over a 30 s period. The curve fittings on the Raman spectra involved the use of a second-order polynomial function for baseline correction and the D and G peak positions were fitted with Lorentzian functions. A conventional XRD instrument was used to characterize and study the microstructure and crystalline phase present in the Cr-DLC films. Transmission electron microscopy (TEM) was used to study in greater details the microstructure of the as-deposited Cr-DLC films. The Hitachi S-3200 N scanning electron microscope was used to observe the interaction between endothelial cells and Cr-DLC films on silicon substrates. The samples were coated with a conducting (Au-Pt) layer of less than 30 nm thickness, using a Polaron-E5000 SEM sample coating unit to reduce surface charging and to obtain a better contrast during SEM-imaging. The conditions used for the SEM-imaging were 5.0 kV and 200× magnification.

2.3 Contact Angle Measurements

Complementary sessile-drop contact-angle measurement was also carried out on the as-deposited films using a KSV CAM 200 optical contact angle meter.

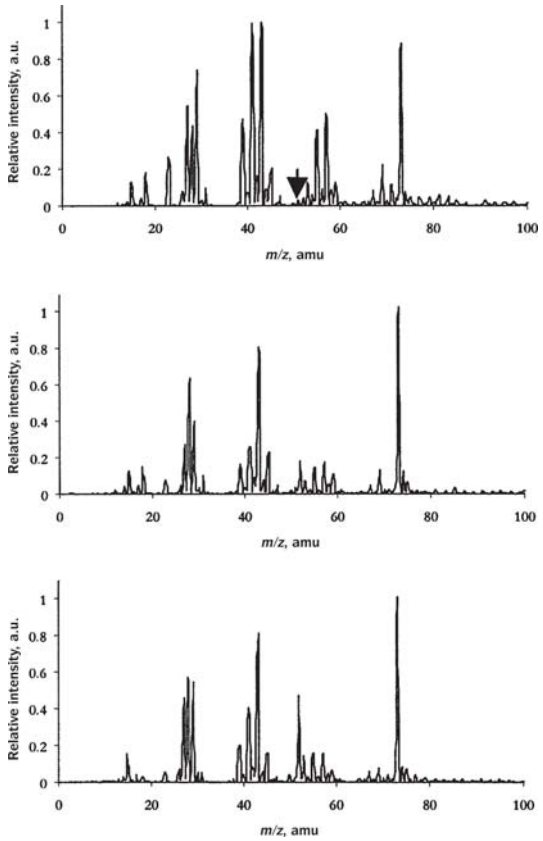

Fig. 2 SIMS spectra for Cr-DLC samples with various Cr contents: (a) 1 at.%, (b) 5 at.%, and (c) 10 at.%

2.4 Cell Culture

Human microvascular endothelial cells were obtained from the molecular biology department of the University of Ulster at Jordanstown, Northern Ireland (U.K.). Cell cultures were maintained in MCDB-131 supplement with L-glutamine (200 mM), 10% fetal calf serum (FCS), epidermal growth factor (EGF) (10 ng/mL), penicillin (20 IU/mL), and streptomycin (20 μg/mL). Cells were grown as monolayers in tissue culture flasks at 37 °C under 5% CO_2/95% air. Proteins were removed with two washings of phosphate buffered saline (PBS). Harvesting of cells for subculturing or tests was performed with a trypsin solution. Subsequently, the trypsin was inactivated with the culture media. Supernatants were separated from the cells by centrifugation. Cells were used when they were about confluent and under the exponential growth phase. The samples were sterilized with 70% ethanol before they were taken into the hood and were given sufficient time to dry. After drying, they were rinsed with PBS or distilled water. Every normal culturing sterility precaution was taken throughout the experiment. About 4×10^5 cells/mL were seeded on top of the Cr-DLC samples placed inside the Petri dishes. The cells on the silicon wafer substrates were fixed with 2.5% glutaraldehyde in 0.1 M phosphate solution for 5 min, followed by 1% osmium tetroxide in 0.1 M phosphate solution for 5 min. The samples were dried with increasing concentrations of ethanol successively and finally with hexamethyldisiloxane (HMDS). Counting of the number of cells over an area of 600 × 400 μm, from recorded SEM image, of various samples were performed using the UTHSCSA ImageTool program developed at the Department of Dental Diagnostic Science, University of Texas

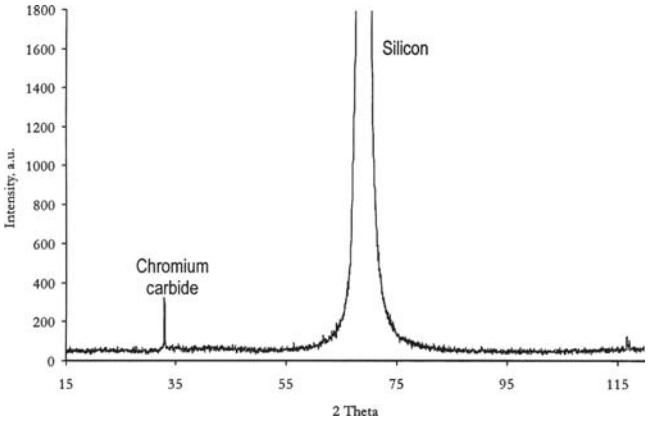

Fig. 3 XRD spectrum for sample 10 at.% Cr-DLC showing the silicon substrate and chromium carbide peaks

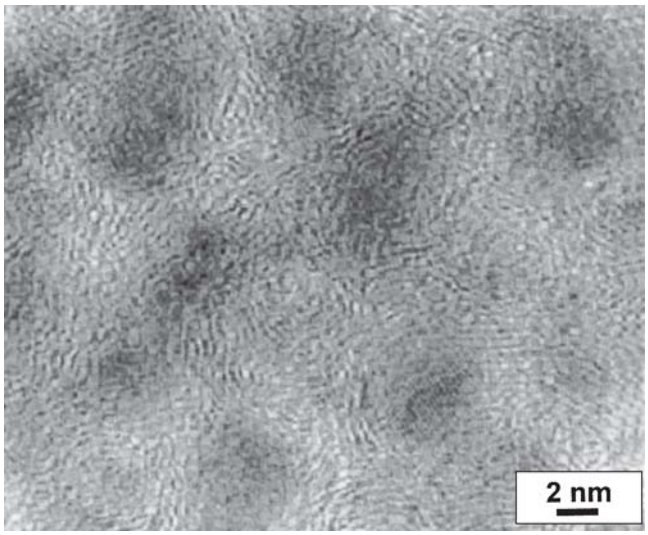

Fig. 4 High-resolution TEM micrograph of the 5 at.% Cr-DLC sample showing the microstructure exhibited by the thin film coating

Table 2 Raman data obtained for the three Cr-DLC samples

m/z (amu)	Ion
15	CH_3^+
16	O^+
18	H_2O^+
23	Na^+
27	$C_2H_3^+$
28	Si^+, CO^+
29	$C_2H_5^+$
31	CH_3O^+
39	$C_3H_3^+$
41	$C_3H_5^+$
43	$C_3H_7^+$, $C_2H_3O^+$
45	$C_2H_5O^+$
52	Cr^+
55	$C_4H_7^+$, $H_3O(H_2O)_2^+$
57	$C_4H_9^+$
59	$C_3H_7O^+$
69	$CrOH^+$, $C_4H_5O^+$
73	$H_3O(H_2O)_3^+$

Note: The data includes I_D and I_G peak intensities; full width at half-maximum (FWHM) values for D and G bands; I_D/I_G ratios and D and G band intensities

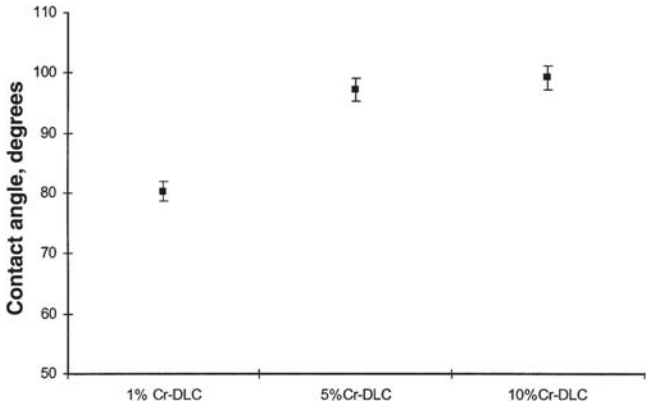

Fig. 5 Graph showing the contact-angle measurements as obtained using the optical method for the three Cr-DLC samples

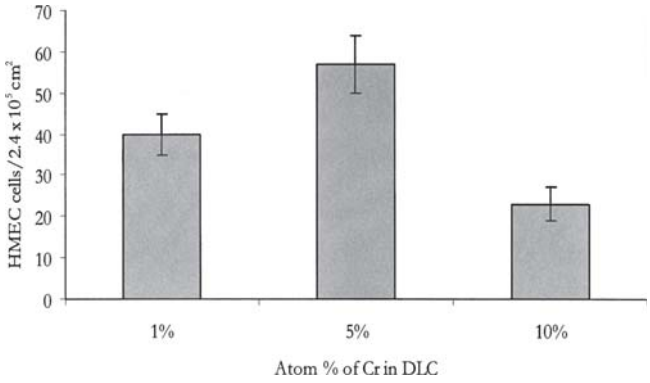

Fig. 6 Graph showing the cell-count results obtained after seeding the human microvascular endothelial cells onto the Cr-DLC surfaces

Table 3 List of ions detected in the three Cr-DLC film samples by SIMS

Sample	%Cr	I_D, a.u.	I_G, a.u.	FWHM, D	FWHM, G	I_D/I_G	D-peak, cm^{-1}	G-peak, cm^{-1}
CrDLC1	1	21.833	21.043	363.68	139.37	1.04	1401.6	1538.8
CrDLC2	5	21.628	20.415	361.08	128.51	1.06	1408.4	1540.6
CrDLC3	10	45.588	49.748	389.90	167.24	0.92	1306.8	1511.8

Health Science Center (San Antonio, TX) by Wilcox et al. (Ref 20).

3. Results and Discussion

Figure 2 shows the SIMS spectra for Cr-DLC samples containing Cr contents of (a) 1, (b) 5, and (c) 10 at.%. It was found from SIMS analysis that different C ions were present in the film samples. The different types of ions detected in the three Cr-DLC film samples by SIMS are displayed in Table 2. The peak corresponding to the Cr^+ ion is shown on the SIMS spectra centered at 52 *m*/*z* (amu) value. The relative intensities of the Cr^+ peaks, centered at 52 *m*/*z* (amu), for 1, 5, and 10 at.% Cr-DLC films were 0.042, 0.18, and 0.46 a.u., respectively. The SIMS data showed that 10 at.% Cr-DLC had the most Cr content out of the three samples and 1 at.% Cr-DLC had the lowest Cr content. RS was used to characterize the quality of the as-deposited Cr-DLC films with different Cr contents, in terms of diamond carbon-phase purity. The data from the RS studies, including intensities of D (I_D) and G (I_G) bands, full width at half-maximum (FWHM) of I_D and I_G bands, I_D/I_G ratio and the positioning of the D and G band peaks can all be found in Table 3. From the Raman investigations, it was found that the Cr-DLC films displayed the two D and G bands of graphite. The G and D bands are usually assigned to a zone center of phonons of E_{2g} symmetry and K-point phonons of A_{1g} symmetry, respectively. The D band peaks for the three Cr-DLC films were positioned at 1401.6, 1408.4, and 1306.8/cm, whereas, the G band peaks were centered at 1538.8, 1540.6, and 1511.8/cm. From both D and G bands, 5 at.% Cr-DLC sample displayed the smallest values for FWHM. The I_D/I_G ratio was the least for 10 at.% Cr-DLC and the highest out of the three samples for the 5 at.% Cr-DLC film. This suggests that there are more disordered graphitic phases in the 5 at.% Cr-DLC sample and the least similar disorder in the 10 at.% Cr-DLC film. Figure 3 shows the XRD spectrum for sample 10 at.% Cr-DLC in the 2θ range from 15° to 115°. It was found from HRTEM studies that the nano-structured Cr-DLC film consisted of nano-sized (5 nm) Cr-carbide particles. The presence of Cr-carbide particles was evident from the XRD peak centered at around 33° 2θ value. The other major intense peak centered at a 2θ value of around 68° corresponds to Si, which was from the Si wafer substrate material. The Cr-carbide nanoparticles were embedded deep into the amorphous DLC matrix and were not present on the DLC surface. This enabled the nanoparticles to be protected by the amorphous DLC film. Figure 4 displays the high-resolution (HRTEM) micrograph representing 5 at.% Cr-DLC and showing the microstructure exhibited by the same as-deposited film. The micrograph shows the presence of nanoclusters (NCs) around 5 nm in diameter surrounded by a ~2 nm thick amorphous matrix. Electron diffraction showed that the dark contrast NCs correspond to Cr carbide, encapsulated by an amorphous matrix. The contact angle measurements obtained using the optical method are as shown in Fig. 5. Chromium doping leads to a gradual increase in the contact angles, as shown in Fig. 5. The increase begins to level out with Cr content above 5 at.%, where it begins to reach a saturation point. The average contact angles displayed by samples 1 at.%, 5 at.%, and 10 at.% Cr-DLC samples were calculated to be 80.285°, 97.23°, and 99.274°, respectively. The results of the cell count analysis shown in Fig. 6 gives an indication of the influence of Cr content in Cr-DLC films on the adherent cell population of the three samples, 5 at.% Cr-DLC provided the best conditions for HMV-EC seeding, while 10 at.% Cr-DLC film resulted in the least population of adherent human endothelial cells onto its surface. It should be noted that sample 1 at.% Cr-DLC was a better base material for seeding endothelial cells than 10 at.% Cr-DLC. Figure 7 displays the SEM micrographs showing the population of endothelial cell attachment onto 1 at.% Cr-, 5 at.% Cr-, and 10 at.% Cr-DLC film surfaces. All three films displayed smooth surface profiles, which is a key requirement in artificial heart valve applications. Surface roughness causes

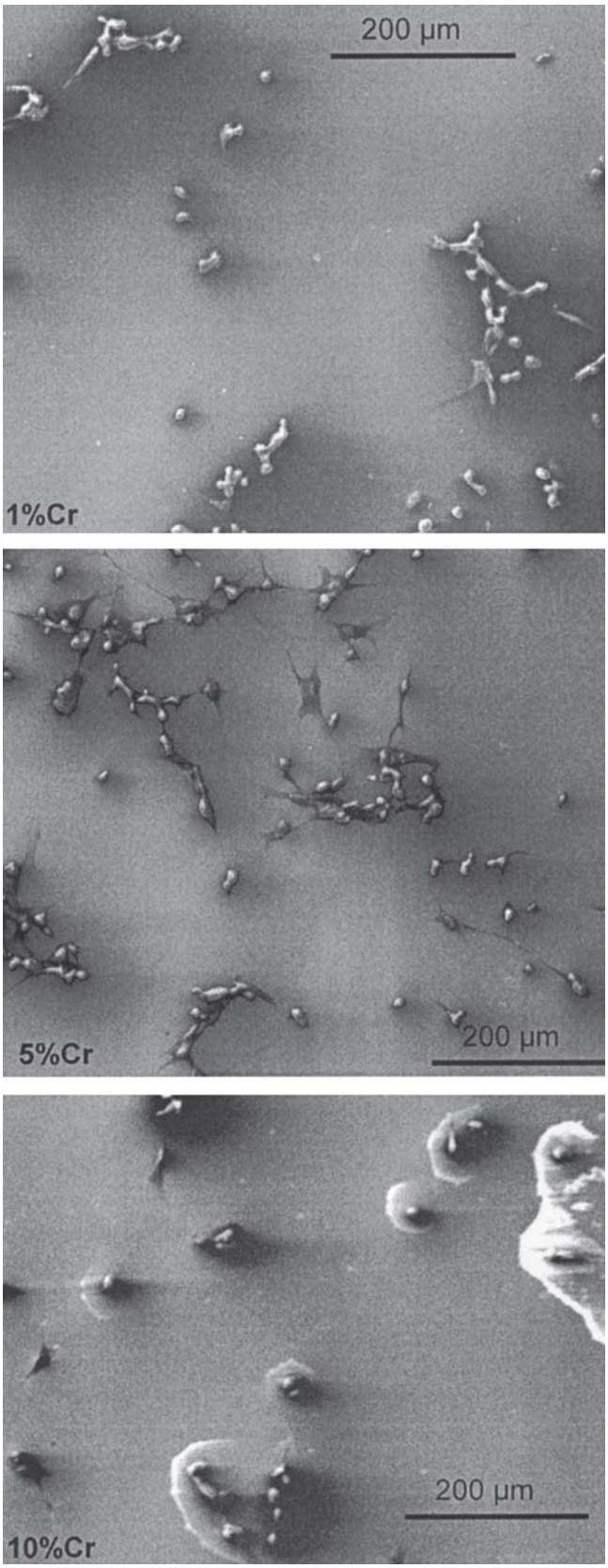

Fig. 7 SEM micrographs showing endothelial cell seeding on the three types of Cr-DLC film surfaces

turbulence in the blood, which leads to red cells being damaged, bacteria adhering, blood coagulating, and clotting. It was noted that there was a direct correlation between the I_D/I_G ratio and the population of endothelial cells attaching to the three Cr-DLC films with different Cr contents. From the three Cr-DLC films, it was observed that the highest value displayed for the I_D/I_G ratio was by 5 at.% Cr-DLC film, which also gave the highest adherent cell population onto its surface. The lowest I_D/I_G ratio value was for 10 at.% Cr-DLC, which showed the least, from the three samples investigated in this study, population of cell attachment to its surface after conducting the cell seeding procedures. It is apparent that increased Cr content into the growing DLC films alters the microstructure of the deposited films. Furthermore, the density of nano-sized Cr-carbide particles produced during film growth is expected to be greatest in 10 at.% Cr-DLC and smallest in the 1 at.% Cr-DLC sample. This difference in the Cr-carbide content in the three films is sure to influence the surface chemistry of the DLC films. It was difficult to correlate the water contact-angle results with the cell-seeding efficiency of the films. However, Grinnell (Ref 20) reported that wettable (hydrophilic) surfaces tend to be more conducive to cell adhesion than similar hydrophobic surfaces. In a recent study by the authors (unpublished results), it was observed that more hydrophobic surfaces containing increasing amounts of Si in Si-DLC films and increasing contact angle with water, tend to promote human endothelial cell growth and adhesion on the films.

4. Conclusions

Cr-DLC films were deposited onto silicon wafers using a magnetron sputtering process, which utilized the intensified plasma-assisted processing system. The as-deposited films contained different amounts of Cr into their microstructure, as confirmed by the SIMS technique. The contact-angle measurements showed that the surface contact angle gradually increased with the percentage Cr content in the films and began to level off at around 10 at.% Cr content. Raman spectroscopy was used to characterize the D and G bands present in all the Cr-DLC films. The FWHM values for the two bands and the I_D/I_G ratios were calculated. The I_D/I_G ratios were correlated to the population of endothelial cell attachments onto Cr-DLC surfaces. High values of the I_D/I_G ratio correlate with better HMC-EC attachment to 5 at.% Cr-DLC film. This finding suggests that disordered graphitic phases in the DLC film lead to enhancement in the seeding of endothelial cells. The authors are working on testing Cr-DLC films for endothelial cell attachment behavior with 2, 3, 4, and 4.5 at.% Cr content.

References

1. K. Barton, A. Campbell, J.A. Chinn, C.D. Griffin, D.H. Anderson, K. Klein, M.A. Moore, and C. Zapanta, Biocompatibility of Diamond and DLC Films, *Biomed. Eng. Soc. (BMES) Bull.,* 2001, **25**(1), p 3-7
2. F.Z. Cui and D.J. Li, A Review of Biocompatibility of Diamond, DLC and CN Films, *Surf. Coat. Technol.,* 2000, **131,** p 481-487
3. J. McLaughlin, B. Meenan, P. Maguire, and N. Jamieson, Properties of DLC Thin Films on Stainless Steel Medical Guidewires, *Diamond Relat. Mater.,* 1996, **5,** p 486-491
4. M.I. Jones, I.R. McColl, D.M. Grant, K.G. Parker, and T.L. Parker, Haemocompatability of DLC and TiC/TiN Interlayers on Titanium, *Diamond Relat. Mater.,* 1999, **8,** p 457-462
5. A. Thomson, F.G. Law, N. Rushton, and J. Franks, Biocompatibility of DLC Coatings, *Biomaterials,* 1991, **12**(1), p 37-40
6. I. Dion, C.H. Roquey, E. Baudet, B. Basse, and N. More, Biocompatibility of Diamond and DLC Coatings on Titanium, *Biomed. Mater. Eng.,* 1993, **3,** p 51-56
7. T.I.T. Okpalugo, A.A. Ogwu, P.D. Maguire, and J.A.D. McLaughlin,

Adhesion of Diamond to Steel and Copper with Titanium Interlayers, *Diamond Relat. Mater.,* 2004, **13,** p 1549-1552
8. P. Yang, N. Huang, Y.X. Leng, J.Y. Chen, H. Sun, J. Wang, F. Chen, and P.K. Chu, In-Vivo Study of Ti-O films, *Surf. Coat. Technol.,* 2002, **156,** p 284-288
9. J.Y. Chen, Y.X. Leng, X.B. Tian, L.P. Wang, N. Huang, P.K. Chu, and P. Yang, Antirhombogenic Study of Surface Energy and Wetting of Titanium Thin Films, *Biomaterials,* 2002, **23,** p 2545-2552
10. Y.X. Leng, H. Sun, P. Yang, J.Y. Chen, J. Wang, G.J. Wan, N. Huang, X.B. Tian, L.P. Wang, and P.K. Chu, Biomedical Properties of TaN Films Synthesized by Reactive Magnetron Sputtering, *Thin Solid Films,* 2001, **398-399,** p 471-475
11. Y.X. Leng, P. Yang, J.Y. Chen, H. Sun, J. Wang, G.J. Wang, N. Huang, X.B. Tian, and P.K. Chu, Fabrication of Ti-O/TiN Coatings on Biomedical Ti Alloys by Metal Plasma Immersion Ion Implantation, *Surf. Coat. Technol.,* 2001, **138,** p 296-300
12. J. Li, Behaviour of Ti and Ti-Based Ceramics in-Vivo and in-Vitro, *Biomaterials,* 1993, **14,** p 229-232
13. A.M. Seifalian, A. Tiwari, G. Hamilton, and H.J. Salacinski, In Vitro Assessment of Cell Adhesion to Biomaterials, *Artif. Organs,* 2002, **26,** p 307-320
14. S.L. Goodman, K.S. Tweden, and R.M. Albrecht, Amorphous Phase and Microstructure of Hydroxyapatite Coatings, *J. Biomed. Mater. Res.,* 1996, **32,** p 249-258
15. V. Pesakova, Z. Klezl, K. Balik, and M. Adam, TiN Coatings: Surface Characterization and Haemocompatability, *J. Mater. Sci.: Mater. Med.,* 2000, **11**(12), p 793-798
16. G.M. Bruinsma, H.C. Van der Mei, and H.J. Busscher, Bacterial Adhesion to the Surfaces of Contact Lenses, *Biomaterials,* 2001, **22,** p 3217-3224
17. A. Ahluwalia, G. Basta, F. Chiellini, D. Ricci, and G. Vozzi, Adhesion of Cells to Certain Biomedical Materials, *J. Mater. Sci.: Mater. Med.,* 2001, **12**(7), p 613-619
18. P.B. Van Wachem, J.M. Schakenraad, J. Feijen, T. Beugeling, W.G. Van Aken, E.H. Blauuw, P. Nieuwenhius, and I. Molenaar, Adhesion and Spreading of Cultured Endothelial Cells on Modified PET: A Morphological Study, *Biomaterials,* 1989, **10,** p 532-539
19. A.A. Adjaottor, E. Ma, and E.I. Meletis, On the Mechanism of Intensified Plasma-Assisted Processing, *Surf. Coat. Technol.,* 1997, **89,** p 197-203
20. F. Grinnell, Cell Spreading Factor: Occurrence and Specificity of Action, *Int. Rev. Cytol.,* 1978, **53,** p 65-144